Factors That Affect the Degree of Twist in β-Sheet Structures: A Molecular Dynamics Simulation Study of a Cross-β Filament of the GNNQQNY Peptide

Xavier Periole,*,† Aldo Rampioni,† Michele Vendruscolo,‡ and Alan E. Mark§

Groningen Biomolecular Sciences and Biotechnology Institute (GBB), Department of Biophysical Chemistry, University of Groningen, Nijenborgh 4, 9747AG Groningen, The Netherlands, Department of Chemistry, University of Cambridge, Lensfield Road, Cambridge CB2 1EW, United Kingdom, and School of Molecular and Microbiological Sciences and the Institute of Molecular Biosciences, University of Queensland, St Lucia, QLD 4072, Australia

Received: September 3, 2008; Revised Manuscript Received: November 10, 2008

By exploiting the recent availability of the crystal structure of a cross-β filament of the GNNQQNY peptide fragment of the yeast prion protein Sup35, possible factors affecting the twisting of β-sheets structures have been analyzed. The advantage of this system is that it is composed entirely of β-sheet and thus free of potential ambiguities present in systems studied previously. In the crystal the cross-β filament consists of antiparallel β-sheets formed by parallel and in register peptides lying perpendicular to the long axis of the filament. The results of a series of molecular dynamics simulations performed under different conditions indicate that in the absence of crystal packing interactions there is no free energy barrier against twisting for the cross-β filament found planar in the crystal. More specifically, we find that there is only a small change in enthalpy (<3 kJ mol^{-1} per residue) for twists in the range 0−12 degrees with the planar form (in the crystal environment) being enthalpically stabilized. In contrast, entropic contributions, in particular those associated with an increase in backbone dynamics upon twisting, stabilize the twisted form. The degree of twist was found to vary depending on the environmental conditions as the result from an apparent subtle interplay of multiple small contributions. These observations are consistent with the different degrees of twist observed in β-sheets both in native protein structures and amyloid fibrils.

Introduction

Understanding the origin of the widespread appearance of a twist in β-sheets in protein structures has challenged researchers in structural biology for more than 30 years.[1] Factors that have been considered include the entropy associated with the backbone degrees of freedom,[1] the out-of-plane deformation of peptide groups,[2] intrastrand,[3,4] and tertiary interaction.[5,6] Although these early theoretical and computational studies were limited to small model systems often lacking the explicit contribution of the solvent, they brought significant insights into the many possible factors likely involved in the twist of β-sheets. More recently, first principle calculations on small single and double stranded antiparallel β-sheets pointed out a tendency of the $C^{\alpha}-C$ bond in the peptide backbone to eclipse the lone pair of the N atom, therefore giving rise to the right-handed twist of the peptide backbone in β-sheets.[7] In a single strand, this effect would be masked by weak intrastrand H-bonds and would only be unleashed when interstrand hydrogen bonding is present.[7] It is also interesting to note that an extensive analysis of a large number of β-sheet structures supported a model in which the degree of twist was determined by the tendency to minimize the surface area of the system.[8]

In this work, we take advantage of the opportunity provided by the recent availability of the structure of a two-stranded cross-β filament formed by a seven-residue peptide fragment (GNNQQNY) from the yeast prion protein Sup35, which was determined using X-ray diffraction.[9,10] This structure provides an atomic resolution model for the three-dimensional packing of peptides within an amyloid fibril.[9] The unit cell in the crystal was found to consist of a tightly packed double layer of complementary β-sheets with closely interlocked side chains. The two β-sheets are aligned in an antiparallel arrangement with the individual peptides lying perpendicular to the long axis of the cross-β filament. Within each β-sheet, the peptides were found to be parallel and in register (Figure 1a). Because of the absence in this structure of the additional factors that may influence β-sheet stability that are unavoidably present in the structures of native states of proteins, this model system was chosen to bring new insights into our understanding of the forces that affect twisting in β-sheets in native states and in amyloid structures of proteins.

A notable feature of this structure, which consists of an extremely regular double-stranded β-sheet, is that it is planar in the crystal. A range of experimental data indicates that fibrils, composed of several copies of cross-β structures or protofilaments, are in general twisted with a degree of twist varying with the morphology of the fibril. Indeed molecular dynamics simulations suggest that the GNNQQNY cross-β filament readily twists when free in solution,[11] as found for other fibrillar systems[12−14] and most β-sheet structures in native proteins.[1]

A detailed analysis of molecular dynamics simulations of the cross-β filament formed by 40 copies of the peptide GNNQQNY[9] under a range of conditions has been performed with the aim of identifying the forces that affect the twist of β-sheets. Being composed exclusively of β-sheet this system avoids the ambiguities inherent in previous studies based largely on native proteins or dipeptides. In particular this system allows the

* To whom correspondence should be addressed. E-mail: x.periole@rug.nl. Tel: +31-503634329. Fax: +31-503634398.
† University of Groningen.
‡ University of Cambridge.
§ University of Queensland.

10.1021/jp8078259 CCC: $40.75
Published on Web 01/20/2009

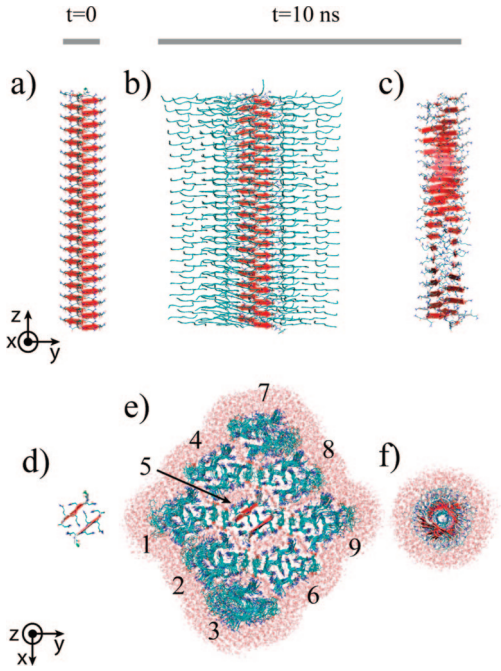

Figure 1. Comparison of the three cross-β filament structures formed by the GNNQQNY peptide fragment of Sup35 that were analyzed in this work. (a−c) Views perpendicular to the filament axis. (d−f) Views along the filament axis; the structures are comprised of 20 peptide pairs. (a,d) Structures determined by X-ray crystallography,[9] (b,e) in a microcrystal environment modeled by a 3 × 3 array of cross-β filaments, and (c,f) in aqueous environment. A solvation shell is shown in e and f.

simultaneous and consistent evaluation of a series of factors in a realistic environment. Moreover the averaging inherent in using 20 peptides in each β-sheet has allowed the magnitude of different factors to be assessed quantitatively. Most notably, we find that rather than reflecting a unique contribution, the degree of twisting of the cross-β structure in aqueous solution results from a subtle combination of multiple factors. The presence of solvent appears to favor the twisted form, although it was not possible to detect a significant change in either the dynamics or the order within the solvent on twisting. Our results also indicate that there is little change in enthalpy within the core of the structure for twists ranging from 0 to 12° with the planar form in the crystal having the lower enthalpy if the interactions between the charged termini are ignored. In contrast entropic contributions were found to favor the twisted form.

Methods

Models of the GNNQQNY Cross-β Filament. The structure of the peptide GNNQQNY[9] was taken from the Protein Data Bank (entry 1yjp). The various systems simulated were constructed using the lattice parameters (a = 21.937, b = 4.866, c = 23.477; α = 90.00, β = 107.08, γ = 90.00) and space group ($P2_1$: $P12_11$) reported for the crystal.[9] A basic unit containing a pair of peptides related by a 2_1 screw axis was constructed. This unit was replicated along the axis of the fibril (b axis) to form a two-stranded β-sheet structure. This will be referred to as the cross-β filament, with 5, 10, and 20 peptides per sheet labeled 5 × 1, 10 × 1, and 20 × 1, respectively. To generate the multilayered microcrystal, the system 20 × 1 was replicated along the a and c axes, such that the central unit was surrounded by 8 copies of the 20 × 1 unit. This block of 9 units is labeled 20 × 9.

Simulation Details. Each system was placed in a periodic rectangular box. The minimal distance between the solute and the box edges was 1 nm. The systems were solvated in water and energy minimized using a steepest descent algorithm. To further relax the solvent configuration, each system was simulated for 50 ps with all heavy atoms of the peptides positionally restrained followed by 50 ps in which only the heavy atoms of the backbone were restrained. The protonation state of titratable groups in the peptide was as expected at pH 7.0 except for the simulations performed with neutralized termini in which case the NH_3^+ and COO^- groups at the termini were replaced by NH_2 and COOH, respectively. Simulations of the system 20 × 1 were also performed in which position restraints on the C^α atoms were applied to maintain the cross-β filament in a planar conformation. Simulations in vacuo were performed using Langevin dynamics with a friction coefficient of 91 ps^{-1}.[15]

All simulations were performed using the GROMACS simulation package version 3.2[16,17] in conjunction with the GROMOS 43a1 force field.[18] The water molecules were described using the simple point charge[19] (SPC) water model. The solute and solvent were coupled independently to an external temperature bath at 300 K using a Berendsen thermostat[20] with relaxation time of 0.1 ps. In addition, in the system 20 × 9 each of the 9 units was coupled to an independent bath. The pressure was weakly coupled to an external bath at 1 bar using a relaxation time of 1.0 ps.[20] Unless otherwise stated, a 2 fs time step was used for the integration of the equations of motion. In order to examine the system over longer time scales, three simulations (5 × 1-DH, 10 × 1-DH, and 20 × 1-DH) were performed in which polar hydrogens in the peptide were replaced by dummy atoms (DH). This allowed a time step of 4 fs to be used with minimal effects on the dynamic and thermodynamic properties of the system.[21]

Covalent bonds within the peptide were constrained using the LINCS algorithm.[22] The SETTLE[23] algorithm was used to constrain the solvent. Nonbonded interactions were calculated using a twin-range cutoff of 0.8/1.4 nm. The charge-group pair list was updated every 5 time steps. To correct for the truncation of electrostatic interactions beyond the long-range cutoff a reaction-field correction was applied (ε = 78).[24] A summary of the simulations performed in this study is given in Table 1.

Analysis. Unless stated otherwise, analysis was performed using 18 pairs of peptides, that is, the first and last pairs of peptides in the cross-β filament were excluded. In certain cases, when comparisons were made with smaller units, analysis was performed on the central 8 pairs of peptides. In the case of the simulation 20 × 1-Vac, the system was divided into two sets of 10 pairs of peptides, pairs 1−10 and pairs 11−20, from which the central 8 pairs were used for analysis. Note that the form of the cross-β filament was analyzed both in a microcrystalline environment and in aqueous solution. The microcrystalline environment mimics the conditions of the X-ray diffraction experiment,[9] and is free of artificial restraints. The simulations in solution with position restraints applied to C^α atoms were performed in order to maintain the planar form while allowing the side chains of the amino acids to relax to the aqueous environment. This was done in order to be able to separate solvation from crystal packing effects. Structural analysis were performed on trajectories with frames every 10 ps. In cases where time correlation functions were involved, the interval between frames was 5 ps.

Twist Angle. The twist angle was defined as the angle between the vectors C^α(Asn2)-C^α(Gln5) of neighboring peptides within the same β-sheet. The average angle of all possible pairs in a specific structure is reported.

TABLE 1: A Summary of the Simulations Presented in This Study

system	starting structure	DH[a]/Δt(fs)	label	simulation length (ns)	termini	solvent	position restraints	simulation speed[b]
5 × 1	5 × 1	Yes/4	5 × 1-DH[1]	100	Charged	Yes	No	
10 × 1	10 × 1	Yes/4	10 × 1-DH[a]	60	Charged	Yes	No	
20 × 1	20 × 1	Yes/4	20 × 1-DH[a]	50	Charged	Yes	No	
20 × 9	20 × 9	No/2	20 × 9	11	Charged	Yes	No	1
20 × 1	20 × 1-DH[a]/10 ns	No/2	20 × 1	10	Charged	Yes	No	40
20 × 1	20 × 1	No/2	20 × 1-C$^{\alpha}$	11	Charged	Yes	on C$^{\alpha}$	
20 × 1	20 × 1-Cα/10 ns	No/2	20 × 1-freed	10	Charged	Yes	No	
20 × 1	20 × 1	No/2	20 × 1-Neut-C$^{\alpha}$	11	Neutral	Yes	on C$^{\alpha}$	
20 × 1	20 × 1	No/2	20 × 1-Neut	16	Neutral	Yes	No	
20 × 1	20 × 1	No/2	20 × 1-Vac	20	Neutral	No	No	

[a] DH stands for Dummy Hydrogens. [b] The values are in ps/h/CPU based on the used 4 or 8 3.4 GHz Intell-Xeon processors.

Hydrogen Bonds. Two independent approaches were used to score the energetic contributions of backbone−backbone hydrogen bonds. The first approach involved the calculation of the energy of interaction between the atoms involved in a specific hydrogen bond. The GROMOS 43a1 force field does not contain a specific hydrogen bonding term.[18] Instead, hydrogen bonding is accounted for using a combination of van der Waals and electrostatic interactions. For this reason, the interaction between the amino nitrogen and hydrogen (donor) and the carbonyl oxygen and carbon (acceptor) was taken as a measure of the strength of the hydrogen bonding interactions. The second approach used the knowledge-based potential developed by Kortemme et al.[25] as implemented in the ROSETTA package.[26,27] It uses four geometrical parameters (see Figure 1 in ref 25), together with information on the type of secondary structure to which the residue belongs, to generate a score for each hydrogen bond. To determine the overall score for individual backbone−backbone hydrogen bonds, the potential was integrated over the distribution of the four geometrical parameters as sampled in the simulations.

Side-Chain Entropy. The conformational entropy of the side-chains was estimated from the probability of sampling alternative rotameric states as given by the side chain $\chi1$ and $\chi2$ dihedral angles in the simulation according to the expression $-kT\cdot\Sigma[p(\chi1,\chi2)\cdot\log p(\chi1,\chi2)]$, where $p(\chi1,\chi2)$ is the probability of occurrence of a given pair $(\chi1,\chi2)$. The $(\chi1,\chi2)$ space was divided in 5 by 5 degrees grid cells.

Backbone Entropy. The backbone conformational entropy was estimated based on the order parameter of the backbone NH vector[28,29] using the expression proposed by Yang and Kay. This assumes that the order parameter of the NH vector reflects motion within a cone and estimates the associated conformational entropy as $S = k_B \ln[\pi(3 - (1 + 8S_{LZ})^{1/2})]$, where k_B is the Boltzmann constant and S_{LZ} is the Lipari-Szabo model-free order parameter of the same vector.[30] S_{LZ}^2 is the plateau value of the time correlation function $C(t) = P2[\vec{\mu}(\tau)\cdot\vec{\mu}(\tau + t)]$, where P2 is the second order Legendre polynomial and $\vec{\mu}$ the NH vector. In the simulations, the order parameter of NH vectors, S^2, were calculated as $S^2 = 3/2[\langle x^2\rangle^2 + \langle y^2\rangle^2 + \langle z^2\rangle^2 + 2\langle xy\rangle^2 + 2\langle xz\rangle^2 + 2\langle yz\rangle^2] - 1/2$, where x, y, and z are the Cartesian coordinates of the normalized NH vector and <> indicates an ensemble average.[31,32] This approach is statistically more reliable[33] as it does not depend on the convergence of $C(t)$ but of the conformational ensemble. S^2 were extracted from 100 ps windows and averaged over 10 ns simulation with frames every 5 ps. Since we do not compare the calculated S^2 from the simulation to experimental values, but use them as a means to compare two forms of the same system, the effects of the time window on the S^2 values is not a concern here. Note however that the values of S^2 were not sensitive to changes of the time window in the range 100 to 5000 ps and of the time interval between frames from 1 to 5 ps (see Supporting Information, Figure S2). The S^2 of each NH bond vector was calculated and an average value, $<S^2>$, was obtained for each residue of the peptide (2−7, the N-terminus is discarded). The pair of peptides on each side of the filament were not considered in the calculation.

Solvent Accessible Surface Area. The solvent accessible surface area (SASA) was computed using the program Naccess-2.1.1[34] with a probe radius of 0.14 nm. The SASA was calculated for each residue and averaged along the structure and over the entire length of a trajectory.

Energetic Analysis. The enthalpy of the different systems was decomposed into a series terms as defined in the GROMOS-43a1 force field.[18] Note, to exclude the contribution of the N- and C-termini, interaction involving the atoms of the terminal $-NH_3^+$ ($-NH_2$) and $-COO^-$ ($-COOH$) groups were not included in the analysis.

Water Density. The density of water was determined by superimposing a 0.1 nm spaced grid onto the simulation box. The average density of the water within each grid cell was then averaged over a 10 ns period. The region where the density was equal to 1.5 standard deviations (σ) above the average was plotted as an isosurface.

Water Ordering. The ordering of water at the surface of the cross-β structure was estimated by calculating the inner-product of the water dipole and the filament long axis, cos θ. The inner-product was averaged over all water molecules within 0.1 nm slices perpendicular to the filament long axis. The calculations were performed on each β-sheet separately and then averaged. Prior to the calculation the β-sheet was fitted to a reference structure. The analysis was performed considering the 720 water molecules with the smallest distance to the heavy atoms of a β-sheet (~0.45 nm water shell). Ten nanosecond simulations were used.

Water Residence Times. The "residence" time (also referred to as the survival or lifetime) of water molecules at the surface of the cross-β structures was estimated by calculating the time-correlation function of finding a given water molecule at the surface, $S_L(t)$.[35−37] $S_L(t)$ can be expressed for a water molecule j as $S_L^j(t) = 1/(T - t)\sum_{v=0}^{T-t} p_j(v, v + t)$, where the function $p_j(v, v + t)$ takes the value of 1 if the water molecule has remained at the surface of the cross-β structure (within a distance <0.45 nm) for a time t after coming in contact with the surface at time v, and zero otherwise; T is the total time of simulation (10 ns). $S_L^j(t)$ were normalized $S_L^j(t) = S_L^j(t)/S_L^j(0)$ and averaged over all the water molecules: $S_L(t) = 1/N_W \sum_{j=1}^{Nw} S_L^j$, where N_w is the number of water molecules. In this analysis, a time interval of 5 ps was used between the frames. This allows discarding the fast (<5 ps) leave and return of water molecules from the

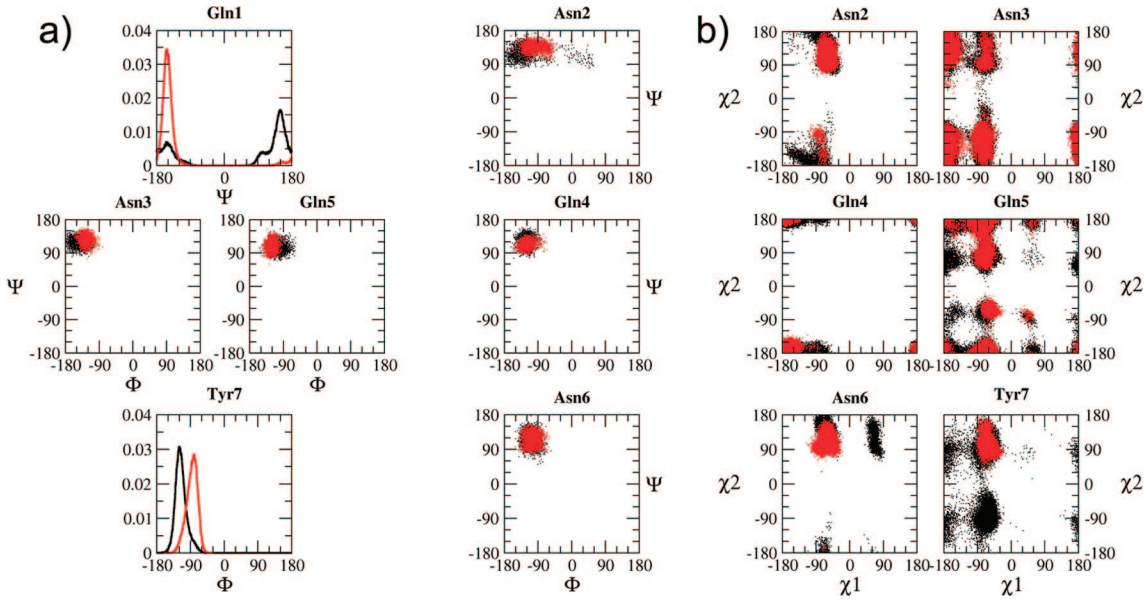

Figure 2. (a) Ramachandran maps for each of the seven residues in the microcrystalline environment (red) and in solution (black). The major changes are observed for Gly1 and Tyr7. The maps were organized to distinguish the residues part of the wet (residues 1, 3, 5, and 7) and dry (residues 2, 4, and 6) interfaces. (b) Maps of the side chain angles $\chi 1$ and $\chi 2$ for each side chain in the GNNQQNY peptide. Rotameric states in the microcrystalline environment (red) and in solution (black) are shown.

shell considered. A stretched exponential was fitted to the resulting curve and used to estimate the average residence-time, τ_L, of water molecule at the surface of the cross-β filament: $S_L(t) \approx \exp[-(t/\tau_L)^\beta]$, where β, the stretching coefficient, gives an indication of the nonexponential trend of the function decay.[35,38]

Rosetta Scoring. The scoring function and the associated weights were used as described by Kulhman et al.[27] in conjunction with the softened repulsive Lennard-Jones potential (soft_rep option).

Results

Cross-β Filament Twist. In order to investigate the effect of crystal-packing on the structure of the cross-β filament formed by the GNNQQNY peptide determined by X-ray crystallography[9] (Figure 1a), two systems were simulated. The first system consisted of nine cross-β filaments arranged in a 3 × 3 array in water, representing a model of a microcrystal; this was used to analyze the properties of a central cross-β filament surrounded by eight other cross-β filaments mimicking a crystal-like environment (Figure 1b). The second system consisted of an individual cross-β filament fully solvated in water (Figure 1c). Within the microcrystal, the cross-β filament retained a planar conformation essentially identical to that observed in the crystal.[9] This result is illustrated in Figure 1b,e, which shows the top and side projections of the microcrystal after 10 ns of simulation. In contrast, the individual cross-β filament in solution rapidly adopted a left-handed twist of 11.6° per peptide along the long axis (Figure 1c,f). This degree of twisting was observed in multiple simulations and was independent of the length of the cross-β filament over the range investigated here (5 to 20 peptide units per β-sheet, data not shown). The value of the twist angle was similar to that observed previously by Esposito et al..[11]

The twisting of the cross-β filament is associated with relatively small structural changes within the individual peptides. The average structure of the peptide in the twisted form deviates from the crystal structure by 1.0 and 0.4 Å (rmsd) for the backbone atoms of residues 1−7 and 2−6, respectively. The

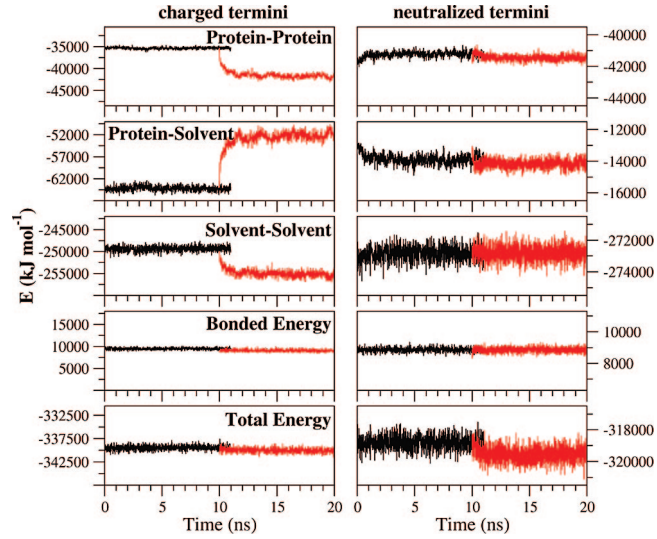

Figure 3. Time series of the bonded and nonbonded potential energy terms (protein−protein, protein−solvent, and solvent−solvent) associated with the structural reorganization of the cross-β filament upon twisting. The cases with charged (left) and neutralized (right) termini are shown using different scales. At the time t = 10 ns the positional restraints applied to the backbone atoms were released.

changes in the backbone dihedral angles are all under 30° and primarily involve Gly1, Asn2, and Tyr7 (Figure 2a). The change in the ψ angle of Gly1 and the φ angle of Asn2 results in a slight elongation of the peptide backbone (data not shown).

Total Energy of the Cross-β Filament. The time evolution of the bonded and nonbonded energy terms was monitored upon the release of the positional restraints placed on the cross-β filament to maintain it in a planar conformation in solution (Figure 3). A major redistribution of the nonbonded energy terms was observed, and both the protein−protein (−157 kJ mol^{-1} per peptide) and the solvent−solvent (−144 kJ mol^{-1} per peptide) interactions became more favorable (i.e., more negative) upon the twisting of the cross-β filament. In contrast, the protein−solvent interactions became less favorable (i.e., less negative, +297 kJ mol^{-1} per peptide). The bonded terms did

TABLE 2: Decomposition of the Intramolecular Potential Energy[a] Extracted from the Molecular Dynamics Simulations of a Cross-β Filament Performed in Different Environments

interaction type		water[b]		microcrystalline[c]		neutral termini in water[d]		neutral termini planar[d]	
bonded		228 ± 9		226 ± 6		221 ± 4		221 ± 3	
			(no termini)[e]		(no termini)[e]		(no termini)[e]		(no termini)[e]
nonbonded	elec	−750 ± 9	**(−824 ± 4)**	−601 ± 5	**(−847 ± 4)**	−752 ± 4	**(−826 ± 4)**	−745 ± 4	**(−828 ± 4)**
	vdW	−278 ± 2	**(−255 ± 2)**	−277 ± 2	**(−257 ± 2)**	−283 ± 3	**(−258 ± 3)**	−282 ± 2	**(−256 ± 2)**
	total	−1028 ± 10	**(−1087 ± 4)**	−878 ± 5	**(−1104 ± 3)**	−1034 ± 4	**(−1084 ± 4)**	−1027 ± 4	**(−1085 ± 4)**
total energy		−800 ± 12		−652 ± 7		−813 ± 4		−807 ± 4	

[a] The potential energy terms correspond to a cross-β filament containing two β-sheets of 20 peptides each. The energies were averaged over the central 18 peptide pairs and given in kJ mol^{-1} per peptide ± one standard deviation. [b] Fully solvated cross-β filament. [c] Cross-β filament in the microcrystalline environment. [d] Fully solvated cross-β filament with neutralized termini. [e] Energies calculated excluding the contributions from the N- and C-termini.

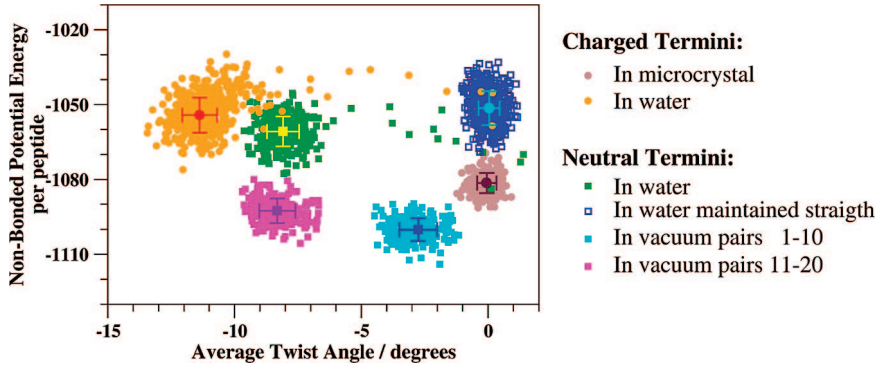

Figure 4. Intramolecular potential energy as a function of twist angle. The intramolecular potential energy (nonbonded terms) versus the average twist angle is plotted for the cross-β filament simulated under different conditions. Each point corresponds to a conformation in a given simulation. The contributions of the termini (charged or neutral) to the energy were excluded. The energy per peptide was averaged over the central eight peptide pairs for all simulations, except those performed in vacuo. In this case, the cross-β filament was divided into two sections each containing 10 peptide pairs from which the central 8 peptide pairs were used for the analysis. The apparent discrepancy between the values shown here and in Table 1 results from the consideration of different number of pairs of peptides, which account for different internal and interactions energies.

not vary significantly. Note that the solvent does not contribute to the bonded term as the geometry of the solvent molecules is fixed. The total potential energy of the cross-β filament in solution was lower by approximately 576 kJ mol^{-1} in the twisted form as compared to the planar conformation, a value that was close to the potential energy of the position restraining term in the restrained simulation (554 ± 32 kJ mol^{-1}).

Internal Energy. A decomposition of the average internal potential energy of the cross-β filament per peptide for the planar (microcrystalline) and twisted (water) configurations is shown in Table 2. The difference in the bonded interactions (angles plus dihedral angles) and in the van der Waals interactions, 2 and 1 kJ mol^{-1} respectively, is well within the statistical uncertainty of our results. However, there was a large electrostatic contribution of about 150 kJ mol^{-1} per peptide that favors the twisted form. This difference is primarily due to interactions between the N- and C-terminal residues (Table 2). Radial distribution functions (see Supporting Information, Figure S1) calculated between the termini of the peptides show that intra, N/N and C/C, and inter-β-sheet, N/C, termini distances change upon twisting. The N/N and C/C distances increase while the N/C distance decreases. The energy associated with the change of the N/C distance contributes to ∼2/3 of the energy difference (data not shown). To determine if the electrostatic charges on the termini were responsible for the twist, simulations were performed in which these charges were neutralized by replacing the NH_3^+ and COO^- groups at the termini by NH2 and COOH. In the simulations of the neutral cross-β filament the average twist angle was reduced by about 30% (from ∼11.6 to ∼8.5°) (Figure 4). Esposito et al.[11] have also noted the twisting of the cross-β filament with neutralized termini. Notably, the neutralization of the end groups had almost no effect on the total internal energy of the peptide (Table 2). Although, the bonded terms and the van der Waals interactions are slightly more favorable, the net contribution of the electrostatic interactions is effectively unchanged. This last aspect may seem surprising. It can however be readily understood by noting that since the cross-β filament is formed by an antiparallel arrangement of parallel β-sheets (Figure 1), the N and C termini of different peptides are in close proximity (see Supporting Information, Figure S1). This leads to an almost complete compensation of the attractive and repulsive energetic terms involving the charges on the termini. These results are consistent with those obtained by excluding the interactions involving the termini (shown in bold in Table 2).

The effect of the presence of charges on the termini is most evident if one compares the simulations of the cross-β filament with the charged and neutralized termini free in solution with simulations in which the C^α atoms were positionally restrained to maintain the planarity of the system. Whereas there is a significant redistribution of energy in the case of the charged termini upon release of the position restraints there is almost no redistribution of energy between the protein−protein, solvent−solvent, and protein−solvent interactions in the case of the neutralized termini (Figure 3). Moreover, the internal energy of the cross-β filament with neutralized termini is virtually identical in the planar and twisted conformations after removal of the termini contribution (Table 2). It is important to note that within the microcrystal environment the enthalpy of the cross-β filament without the termini contribution relaxes by about 20 kJ mol^{-1} per peptide when compared to the planar form with both charged and neutral termini.

Taken together, these results indicate that there is very little change in the total enthalpy of the system upon twisting with

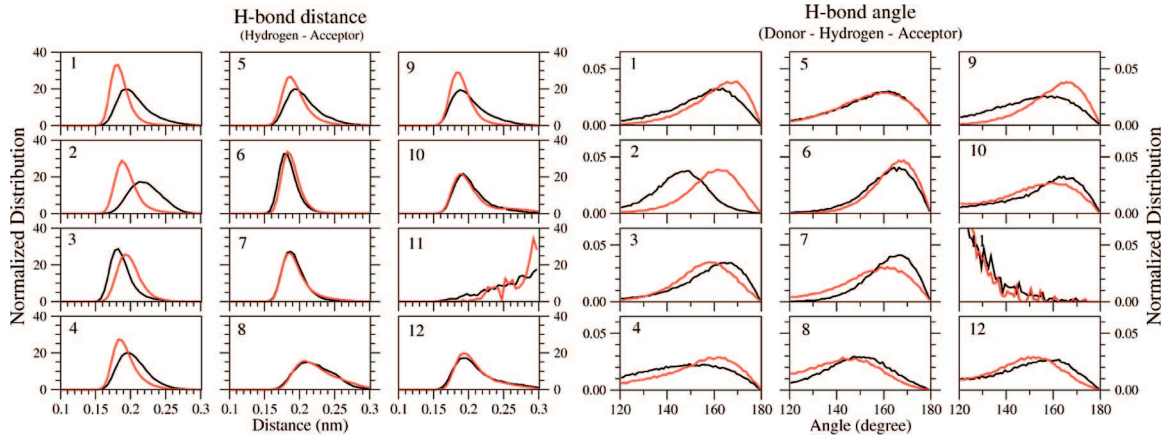

Figure 5. Probability distribution histograms of the hydrogen−acceptor distances and donor−hydrogen−acceptor angles for 12 hydrogen bonds identified in the X-ray crystal structure,[9] in the microcrystalline environment (red), and in solution (black). The H-bonds 1 to 5 are backbone−backbone H-bonds between Asn2-O and Asn3-H/N, Gln4-N/H and Asn3-O, Gln4-O and Gln5-H/N, and Asn6-N/H and Gln5-O, and Asn6-O and Tyr7-H/N, respectively. The H-bonds 6 to 12 are side chain-side chain H-bonds between Gln4-OE1 and Gln4-NE2/HE21, Asn6-ND2/HD21 and Asn6-OD1, Asn2-ND2/HD21 and Asn2-OD1, Asn2 N/H and Asn2-OD1, Asn3-OD1 and Asn3-ND2/HD21, Asn3-ND2/HD22 and Gln5-OE1, and Gln5-NE2/HE21 and TYR7-OH.

TABLE 3: Energy of the Backbone−Backbone Hydrogen Bonds (kJ mol^{-1} per Peptide)

hydrogen bond #	1	2	3	4	5	Σ
GROMOS[a]						
water	−9.6	−8.5	−9.6	−8.6	−9.5	−45.9
microcrystal	−10.5	−10.8	−10.4	−9.3	−9.7	−50.6
water-microcrystal	+0.8	+2.3	+0.7	+0.6	+0.2	+4.7
Rosetta[b]						
water	−12.6	−5.9	−16.7	−11.1	−12.9	−59.2
microcrystal	−18.9	−19.3	−16.5	−15.1	−14.9	−84.7
water-microcrystal	+6.3	+13.3	−0.1	+4.1	+2.1	+25.6

[a] Sum of the electrostatic and van der Waals terms involving the C═O (donor) and N−H (acceptor) vectors in the GROMOS 43a1 force field.[18] [b] Energy calculated according to the hydrogen bonding knowledge-based potential[25] used in the ROSETTA software.[26,27]

the configuration in the crystal structure having a lower internal potential energy than that of the twisted form once the termini are excluded. Examination of the bonded and nonbonded interactions did not reveal a specific energy term that could be correlated with the twist.

Hydrogen Bonding. Hydrogen bonding interactions play a major role in stabilizing the structures of proteins.[39−41] To monitor differences in the hydrogen bonds between the planar and twisted forms, the distance between the hydrogen and the acceptor atoms, r_{OH}, and the angle between the donor, the hydrogen, and the acceptor atoms, ν, for the hydrogen bonds found in the X-ray model[9] were analyzed (Figure 5). The five backbone−backbone (BB) hydrogen bonds are conserved upon twisting and change only slightly in geometry. To determine if the BB hydrogen bonding interactions favored the planar or the twisted form, the strength of the interaction was calculated by summing the electrostatic and van der Waals interaction energies between the N−H (donor) and C═O (acceptor) vectors as defined in the GROMOS 43a1 force field.[18] Using this criterion the planar configuration was found energetically favored by 4.7 kJ mol^{-1} per peptide (Table 3). The side chain-side chain hydrogen bonds were only marginally affected by the twist (Figure 5). These results suggest that hydrogen bonding does not drive the twist, which is in agreement with previous work suggesting that the optimal hydrogen bonding configuration within a β-sheet is planar rather than twisted.[2]

The contribution of BB hydrogen bonding interactions to the twist was also estimated using the statistical hydrogen bonding potential[25] from ROSETTA using configurations extracted from the simulations. The planar form was again found to be energetically favored (Table 3). The full ROSETTA potential,[26,27] which includes an implicit solvation term, predicted the planar form of the isolated cross-β filament to be more stable than the twisted form (data not shown). Interestingly, the same result was obtained using the GROMOS 43a1 force field[18] in conjunction with an implicit solvent model as described by Fan et al.[42] These observations are consistent with the conclusion that the intramolecular potential energy of an isolated cross-β filament favors the planar configuration (Table 2) and would suggest that entropic effects, which are not fully considered using an implicit representation of the solvent, may play a significant role in driving the twist.

Side-Chain Entropy. Entropic effects due to the amino acid side-chains have been proposed to play an important role in protein folding,[40,43] in particular for stabilizing twisted conformations of β-sheets. An analysis of the distributions of the side-chain $\chi1$ and $\chi2$ dihedral angles showed that the side-chains were more restricted in the microcrystalline environment as compared to fully solvated case (Figure 2b). Thus, the release of the cross-β filament from the microcrystalline environment would lead to favorable entropic terms that could in principle give rise to the twist. To determine the possible magnitude of this contribution the configurational entropy of each side chain was estimated as $-kT\sum(\pi_i \ln \pi_i)$, where π_i is the probability of observing a particular combination, i, of $\chi1$ and $\chi2$ angles for a given side chain during the simulations (see Methods). This approach ignores possible correlations between and within the side chains and thus represents an upper estimate of the possible entropic contribution of the side chains. The gain in entropy at 300 K going from the microcrystalline environment to solution was found to be ∼10 kJ mol^{-1} per peptide. However, between the planar (position restrained) and twisted forms in solution this contribution is reduced to about 2.5 and 3.2 kJ mol^{-1} per peptide for the charged and neutralized termini simulations, respectively. Note that the position restraints applied to the backbone C$^{\alpha}$ atoms might affect the mobility of the side chains. These results suggest that in solution the side chain entropy would marginally favor the twisted form.

Backbone Entropy. To quantify any changes in backbone entropy is problematic as one must attempt to assign a change in entropy to individual residues along the chain. The approach

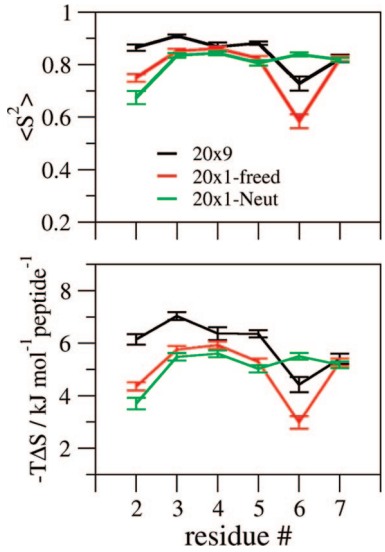

Figure 6. Analysis of the backbone dynamics. (top panel) NH S^2 order parameters and (bottom panel) associated entropies, which were calculated according to the expression derived by Yang and Kay (see Methods). The values presented are averages over all possible 100 ps time windows from the 10 ns simulation with frames every 5 ps, so there is a total of 3600 values for each residue. The two peptide pairs at the ends of the filament were omitted. The error bars indicate one standard error based on the 36 values obtained for each NH vector.

taken here was to compare the dynamics of the backbone NH vectors in the planar and twisted forms. Changes in the dynamics of NH vectors, as can be inferred from NMR relaxation experiments, are commonly used to probe changes in the backbone dynamics of proteins.[44] In addition, expressions have been developed, which relate the NMR-derived order parameter, S_{LZ}^2, of an NH vector to a measure of conformational entropy.[28,29] These approaches are widely used to estimate changes in conformational entropy of the backbone, that is, upon ligand binding.[45] Here S^2 values obtained from the simulations (see Methods) are used to estimate the change in conformational entropy based on the Yang-Kay expression. Figure 6 shows the per-residue NH order parameter, S^2, and the corresponding entropies as a function of the residue number. There is a systematic decrease of the NH order parameter (corresponding to a net increase in spatial mobility) when going from the microcrystal environment (planar) to free in solution (twisted). The resulting change in conformational entropy at 300 K associated with the NH vector of residues 2−7 is 6.2 kJ mol^{-1} per peptide. In the case of the neutralized termini simulation the change in conformational entropy upon twisting is 5.2 kJ mol^{-1} per peptide.

A number of important caveats concerning these estimates should be noted. First, the estimates are based on changes in local motion and are dependent on the assumption of a particular motional model to account for the magnitude of S^2. Second, in the planar form the peptide is heavily restrained by the microcrystalline environment and is not fully equivalent to a planar structure free in solution. Third, this estimate of the conformational entropy neglects possible correlations between the motions of different vectors in the system. In regard to this last point we note that the effects of correlations are likely to be comparable in the planar and twisted forms of the cross-β filament and therefore cancel each other in the comparison.[44] The effect of performing the simulations of the cross-β structure free in solution and in the microcrystal mimic is difficult to quantify. While the presence of neighboring peptides within the

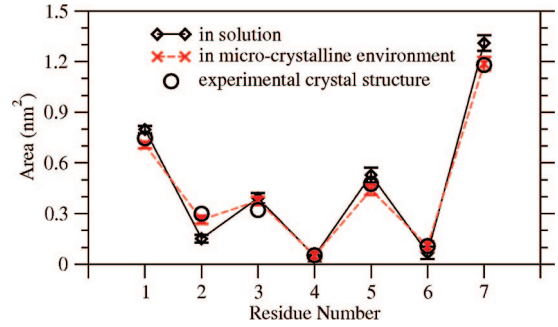

Figure 7. Solvent accessible surface area per residue averaged over the central 18 pairs of peptide of the 20 × 1 system (Table 1) calculated from the starting crystal structure and averaged over the simulations in the microcrystalline and aqueous environments.

cross-β structure will severely restrict side chain motion the effect on the motion of the backbone NH vectors is expected to be small. Nevertheless, global fluctuations in the structure around its equilibrium conformation free in solution will lead to an apparent increase in local motion.

Role of the Solvent. To determine whether the presence of solvent was required for the system to twist, the cross-β filament was simulated in vacuo using Langevin dynamics (20 × 1-Vac, see Table 1). This simulation was performed using neutralized termini as described earlier to avoid charge−charge interactions between the N- and C-termini. Again, the cross-β filament twisted readily in the simulations. However, in contrast to the earlier simulations two distinct regions were observed. The twist of the first 10 peptide pairs was almost identical to that obtained for the peptide with neutralized termini in water (pairs 1−10; Figure 4). The twist in the remaining section of the cross-β filament was smaller (about 3 degrees) (pairs 11−20, Figure 4). The two segments twisted simultaneously. By comparing the simulations of the cross-β filament with neutralized termini in explicit solvent and in vacuo, we see that the process by which the cross-β filament twists is more rapid in the presence of the solvent and that the process is more complete giving rise to a uniform overall twist. Therefore, although the presence of water is not required for the cross-β filament to twist, it does stabilize the twisted form.

Solvent Accessible Surface Area. The change in the solvent accessible surface area (SASA) before and after twisting was calculated for individual residues by comparing the twisted cross-β filament with the cross-β filament obtained by removing and fully solvating the central cross-β filament in the array of nine cross-β filaments making up the microcrystalline model. Only small differences were observed between the planar and the twisted form (Figure 7). The total SASA of the central 18 pairs of peptides increases from 112.75 ± 1.21 nm^2 in the microcrystalline environment to 118.54 ± 0.52 nm^2 for the fully solvated case (twisted). The difference of 5.79 nm^2 corresponds to only 0.16 nm^2 per peptide. For comparison a sphere with a radius of 0.14 nm (commonly used to represent a water molecule) has a surface area of ∼0.25 nm^2. Similar differences were obtained with the planar form of the filament in solution, indicating that the crystalline environment does not affect the SASA of the cross-β filament.

Solvent Ordering. Differences in the degree of order within the water molecules in the vicinity of the cross-β filament in the planar (C^α atoms positionally restrained) and twisted forms (free in solution) with both charged and neutralized termini were quantified by calculating the average of the inner product, $\langle\cos\theta\rangle$, of the water dipole with the long axis of the fibril. Figure 8 shows $\langle\cos\theta\rangle$ for water molecules found within 0.45 nm of

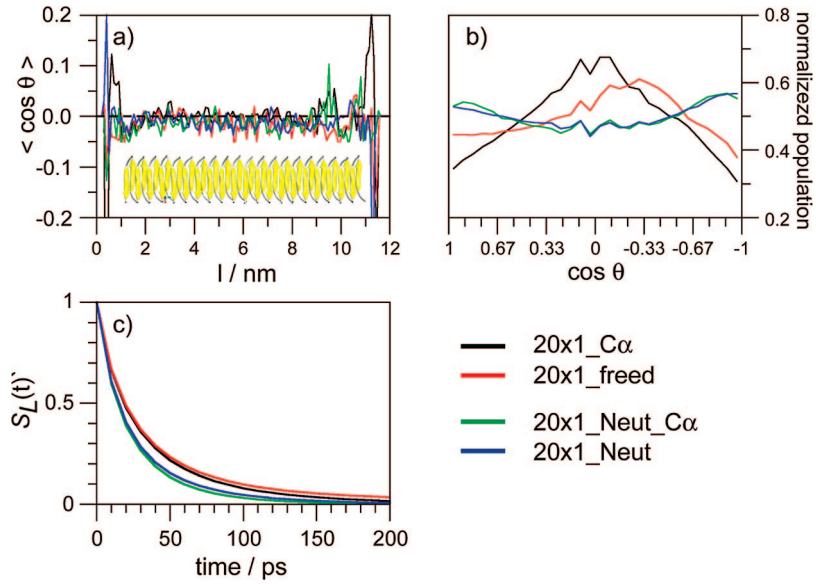

Figure 8. Ordering and dynamics of water molecules at the surface of the cross-β filament. (a) Average of the inner-product (<cos θ>) between a vector aligned along the water dipole and the long axis of the filament; the average is over all water molecules within slices 0.1 nm thick and perpendicular to the long axis of the filament. (b) Probability distribution of the inner-product for the water molecules within the core of the filament (2−10 nm in panel a). (c) Layer-survival-time-correlation function, S_L (see Methods); this function gives the probability that a water molecule remains at surface of the cross-β filament after a time t following its entrance in the surface layer.

the surface of the cross-β filament. As can be seen from Figure 8a the value of <cos θ> fluctuates close to zero along the entire length of the fibril in all four cases. Examination of the distribution of the cos θ values within the central section of the cross-β filament (2−10 nm) revealed that in the case of the charged termini there is a systematic difference in the orientation of the water between the planar and twisted forms of the filament (Figure 8b). Specifically, the predominant orientation of the water dipole changes from ∼90 to ∼70 degrees upon twisting. In the simulations with the neutralized termini the orientation of the water is more equally distributed with the dipole of water lying parallel to the long axis of the structure. In this case the orientation of water surrounding the fibril does not change upon twisting. These results indicate that the presence of charged termini strongly affects the orientation of water molecules around the cross-β filament and is dependent on whether the structure is twisted or not. However, in the case where the termini are neutralized the preference of the water to adopt a specific orientation is less pronounced and does not depend on the degree of twist.

Solvent Dynamics. Changes in solvent dynamics were examined by calculating the average residence time of water molecules in contact with the fibril. The residence times were determined based on an analysis of the time correlation function of finding a water molecule within 0.45 nm of the surface of the cross-β filament (Figure 8c). The decay of these functions is systematically slower in the twisted form as compared to the planar form indicating that, on average, the residence time of water molecules is longer in the twisted form. Fitting these correlation functions with a stretched exponential showed that the changes in residence times of water molecules upon twisting are small: 29.6 and 30.9 ps in the case with charged termini and 21.6 and 22.9 ps in the case with neutral termini. The stretching constants were 0.77, 0.70, 0.83, and 0.79, respectively, showing that similar deviations from pure exponential behavior were observed for all cases. Again the differences between the charged and neutralized termini are greater than the effect of the twist. Taken together these results indicate that the dynamics of the water are only marginally affected by the twisting of the cross-β filament.

Discussion

The simulations show that although the structures of the cross-β filament in water and in the crystal differ noticeably (Figure 1) the changes within each individual peptide upon twisting are small (Figure 2a). The structural changes linked to the twist result in a marked decrease in the intramolecular potential energy. This decrease is associated primarily with electrostatic interactions between the charged termini. If interactions involving the termini are excluded the difference in the intramolecular potential energy favors the planar form (Table 2). A comparison between the results of the simulations in water and in vacuo, in which the termini were neutralized, indicated that the interactions between the charged termini are not required for the cross-β filament to twist. This result is not surprising since many β-sheet structures are observed to twist that do not contain charged termini. Although interactions between the termini are not required for the cross-β filament analyzed here to twist the electrostatic interactions involving the termini do significantly increase the degree of twist (from ∼8.5 to ∼11.6 degrees). In addition, the backbone−backbone hydrogen bonds were found not to favor the twisted form of the cross-β filament in agreement with previous studies.[2] Overall, the results indicate that there is little to no enthalpic cost associated with the twisting of the peptide by an angle ranging from 0 to ∼12 degrees (Figure 4).

The upper bound for the change in the entropy of the side-chains between the planar and twisted forms in solution was estimated to be approximately 2−3 kJ mol^{-1} per peptide. This suggests that in solution the side chain entropy may marginally favor the twisted form. Changes in the backbone NH group order parameters also suggested an increase in the conformational entropy of the backbone on twisting. This may contribute as much as 6 kJ mol^{-1} per peptide to the stabilization of the twisted form. In combination, these results suggest that entropic effects significantly favor the twisted form.

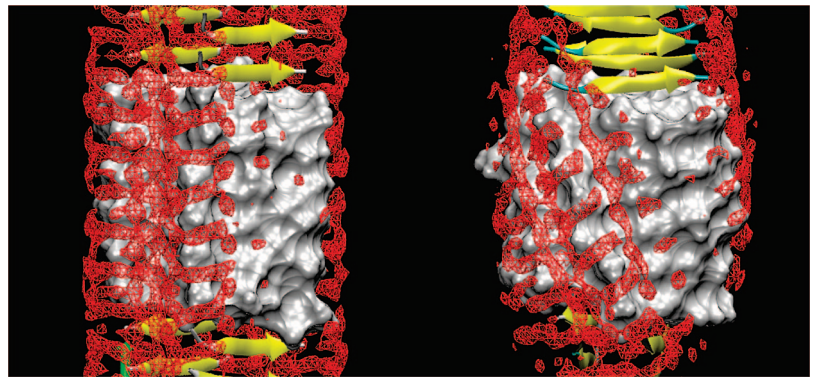

Figure 9. Three-dimensional contour map of the water density surrounding a region of the cross-β filament maintained planar in solution (left) and free in solution (right). The solvent accessible molecular surface of the six central pairs of peptides of the fibril is shown in silver. A cartoon representation of the structure of the cross-β filament is shown above and below the molecular surface. The red wire-frame represents the mass density of the solvent (average plus ~1.5 standard deviation) averaged over 10 ns of simulation. The figure was generated using VMD.[58]

The simulations in vacuo demonstrate that the solvent is not required for the cross-β filament considered here to twist. Nevertheless, the difference between the simulations of the cross-β filament with neutralized termini in vacuo and in water clearly suggests that the presence of solvent favors the twisted form. In this regard we note that there was a small increase in the solvent accessible surface area upon twisting (~60% of a water molecule per peptide), which might relate to the slight decrease of the protein−solvent interaction energy observed in the simulations with neutralized termini. Moreover, using two different implicit solvation models the planar form was predicted to be more stable than the twisted form. These results suggest that the effect of solvent on the relative stability of the planar and twisted forms may be due to differences in the degree of solvent ordering and/or dynamics. While it is not possible to directly determine the change in the entropy of the solvent associated with the transition from the planar to the twisted forms a plot of the water density close to the cross-β filament (Figure 9) reveals that there is a high degree of ordering of the solvent in the proximity of the surface of both the planar and twisted forms. However, while in the charged termini simulations there were marked differences between the planar and twisted forms (Figure 8) this was not evident in the simulations performed with neutralized termini. Moreover, the average residence time of water molecules at the surface of the cross-β filament was only marginally affected by the twist of the structure in both charged and neutralized termini.

The relatively weak dependence of the intramolecular potential energy on the degree of twist (Figure 4) suggests that the cross-β filament formed by the GNNQQNY peptide fragment would readily adopt different degrees of twist depending on the environment. At least in part, this result could explain the different values of the twist observed in amyloid fibrils composed of different numbers of cross-β filaments, and the different morphologies of amyloid fibrils that can be formed under various conditions.[10,22,46−54] For example, in their "correlated twist model" Jimenez et al.[53] propose that the twist of the cross-β filaments follows the twist of the amyloid fibril. The fact that the potential energy changes little as a function of the twist angle (Figure 4) suggests that cross-β filaments could adapt readily to different degrees of overall twist of an amyloid fibril. This in turn could result from different numbers of cross-β filaments being present in the amyloid fibril itself. Different degrees of twist of β-sheet assemblies have been observed when varying the number of layers in the assembly.[14,55,56] We do note, however, that alternative explanations for the appearance of different morphologies have also been proposed[49] and that the effect of pH and/or ionic strength on the fibril morphology[47] is likely to be the result of changes in the delicate balance of intermolecular forces (electrostatic) involved in the fibril formation.[57]

Conclusions

The availability of the crystal structure of a model for the cross-β protofilament formed by the peptide GNNQQNY from the yeast prion protein Sup35[9] provides a unique opportunity to examine in atomic detail the forces that affect the twisting of β-sheets[1] in a large assembly. The cross-β filament[9] was simulated in this work under different external conditions, and was found to remain planar in a microcrystalline environment and to adopt a left-handed twist of about 11.6 degrees around its axis when fully solvated.

Our analysis has shown that there is a small enthalpy penalty (to the core of the cross-β filament) associated with a twist ranging from 0 to 12 degrees per peptide. In contrast, the changes in side-chain and backbone conformational entropy were found to favor the twist. In addition, comparison of simulations in vacuo and in explicit solvent demonstrated that, although not required for the twist to occur, the solvent favors a twisted form of the cross-β filament. Since the overall net magnitude of all the factors that were investigated was small, our results suggest that there is no single dominant term that accounts for the degree of twist in cross-β filaments or likely more generally in β-sheets. Rather, the degree of twist originates from a combination of factors including hydrogen bonding, residue-specific backbone and side-chain electrostatic and van der Waals interactions, entropic contributions associated with side chain packing, backbone dynamics, and solvent reorganization. Among all these factors, a potential contribution from the backbone dynamics was the most appealing. Further investigations will be conducted to quantify more precisely, if possible, the magnitude of these factors which are of great interest in the development of biomaterials.

Acknowledgment. We thank Josy ter Beek for participating in the early stage of this project and Joshua Berringam and Sarah Harris for sharing unpublished data. We are grateful to Hao Fan for providing a version of GROMACS with the implementation of the implicit solvent used in this study. The work was supported by the European Community Training and Mobility of research "Protein (mis)folding", Grant HPRN-CT-2002-00241. The use of the Dutch national supercomputing facilities (SARA) is gratefully acknowledged. The authors declare no conflict of interest.

Note Added after ASAP Publication. This paper was published ASAP on January 20, 2009. A label in Figure 2 was changed. The revised paper was reposted on February 5, 2009.

Supporting Information Available: Radial distribution functions of the peptide termini in different simulation setups and the effect of varying the time interval and averaging window in the calculation of order parameters are given. This material is available free of charge via the Internet at http://pubs.acs.org.

References and Notes

(1) Chothia, C. *J. Mol. Biol.* **1973**, *75*, 295–302.
(2) Salemme, F. R. *Prog. Biophys. Mol. Biol.* **1983**, *42*, 95–133.
(3) Maccallum, P. H.; Poet, R.; Milnerwhite, E. J. *J. Mol. Biol.* **1995**, *248*, 374–384.
(4) Chou, K. C.; Nemethy, G.; Scheraga, H. A. *J. Mol. Biol.* **1983**, *168*, 389–407.
(5) Yang, A. S.; Honig, B. *J. Mol. Biol.* **1995**, *252*, 366–376.
(6) Wang, L.; Oconnell, T.; Tropsha, A.; Hermans, J. *J. Mol. Biol.* **1996**, *262*, 283–93.
(7) Shamovsky, I. L.; Ross, G. M.; Riopelle, R. J. *J. Phys. Chem. B* **2000**, *104*, 11296–11307.
(8) Koh, E.; Kim, T. *Proteins* **2005**, *61*, 559–569.
(9) Nelson, R.; Sawaya, M. R.; Balbirnie, M.; Madsen, A. O.; Riekel, C.; Grothe, R.; Eisenberg, D. *Nature* **2005**, *435*, 773–778.
(10) Sawaya, M. R.; Sambashivan, S.; Nelson, R.; Ivanova, M. I.; Sievers, S. A.; Apostol, M. I.; Thompson, M. J.; Balbirnie, M.; Wiltzius, J. J. W.; McFarlane, H. T.; Madsen, A. O.; Riekel, C.; Eisenberg, D. *Nature* **2007**, *447*, 453–457.
(11) Esposito, L.; Pedone, C.; Vitagliano, L. *Proc. Natl. Acad. Sci. U.S.A.* **2006**, *103*, 11533–11538.
(12) Soto, P.; Cladera, J.; Mark, A. E.; Daura, X. *Angew. Chem., Int. Ed.* **2005**, *44*, 1065–1067.
(13) Rohrig, U. F.; Laio, A.; Tantalo, N.; Parrinello, M.; Petronzio, R. *Biophys. J.* **2006**, *91*, 3217–3229.
(14) Bellesia, G.; Fedorov, M. V.; Timoshenko, E. G. *Physica A* **2007**, *373*, 455–476.
(15) Yun-Yu, S.; Lu, W.; van Gunsteren, W. F. *Mol. Simul.* **1988**, *1*, 369–383.
(16) Berendsen, H. J. C.; van der Spoel, D.; Vandrunen, R. *Comput. Phys. Commun.* **1995**, *91*, 43–56.
(17) Van der Spoel, D.; Lindahl, E.; Hess, B.; Groenhof, G.; Mark, A. E.; Berendsen, H. J. C. *J. Comput. Chem.* **2005**, *26*, 1701–1718.
(18) van Gunsteren, W. F.; Billeter, S. R.; Eising, A. A.; Hunenberger, P. H.; Kruger, P.; Mark, A. E.; Scott, W. R. P.; Tironi, I. G. *Biomolecular Simulation: The GROMOS96 Manual User Guide*; Vdf Hochschulverlag AG an der ETH Zurich and Biomos b.v.: Zurich, 1996.
(19) Berendsen, H. J. C.; Postma, J. P. M.; van Gunsteren, W. F.; Hermans, J. *Interaction model of water in relation to protein hydration*; Reidel: Dordrecht, 1981.
(20) Berendsen, H. J. C.; Postma, J. P. M.; van Gunsteren, W. F.; Dinola, A.; Haak, J. R. *J. Chem. Phys.* **1984**, *81*, 3684–3690.
(21) Feenstra, K. A.; Hess, B.; Berendsen, H. J. C. *J. Comput. Chem.* **1999**, *20*, 786–798.
(22) Hess, B.; Bekker, H.; Berendsen, H. J. C.; Fraaije, J. *J. Comput. Chem.* **1997**, *18*, 1463–1472.
(23) Miyamoto, S.; Kollman, P. A. *J. Comput. Chem.* **1992**, *13*, 952–962.
(24) Tironi, I. G.; Sperb, R.; Smith, P. E.; van Gunsteren, W. F. *J. Chem. Phys.* **1995**, *102*, 5451–5459.
(25) Kortemme, T.; Morozov, A. V.; Baker, D. *J. Mol. Biol.* **2003**, *326*, 1239–1259.
(26) Dantas, G.; Kuhlman, B.; Callender, D.; Wong, M.; Baker, D. *J. Mol. Biol.* **2003**, *332*, 449–460.
(27) Kuhlman, B.; Dantas, G.; Ireton, G. C.; Varani, G.; Stoddard, B. L.; Baker, D. *Science* **2003**, *302*, 1364–1368.
(28) Akke, M.; Bruschweiler, R.; Palmer, A. G. *J. Am. Chem. Soc.* **1993**, *115*, 9832–9833.
(29) Yang, D. W.; Kay, L. E. *J. Mol. Biol.* **1996**, *263*, 369–382.
(30) Lipari, G.; Szabo, A. *J. Am. Chem. Soc.* **1982**, *104*, 4546–4559.
(31) Smith, L. J.; Mark, A. E.; Dobson, C. M.; van Gunsteren, W. F. *Biochemistry* **1995**, *34*, 10918–10931.
(32) Hu, H.; Hermans, J.; Lee, A. L. *J. Biomol. NMR* **2005**, *32*, 151–162.
(33) Chandrasekhar, I.; Clore, G. M.; Szabo, A.; Gronenborn, A. M.; Brooks, B. R. *J. Mol. Biol.* **1992**, *226*, 239–250.
(34) Hubbard, S. J.; Thornton, J. M. NACCESS, Computer Program; Department of Biochemistry and Molecular Biology, University College London, 1993.
(35) Rocchi, C.; Bizzarri, A. R.; Cannistraro, S. *Phys. Rev. E* **1998**, *57*, 3315–3325.
(36) Garcia, A. E.; Stiller, L. *J. Comput. Chem.* **1993**, *14*, 1396–1406.
(37) Brunne, R. M.; Liepinsh, E.; Otting, G.; Wuthrich, K.; van Gunsteren, W. F. *J. Mol. Biol.* **1993**, *231*, 1040–1048.
(38) Bizzarri, A. R.; Cannistraro, S. *J. Phys. Chem. B* **2002**, *106*, 6617–6633.
(39) Stickle, D. F.; Presta, L. G.; Dill, K. A.; Rose, G. D. *J. Mol. Biol.* **1992**, *226*, 1143–1159.
(40) Avbelj, F.; Fele, L. *J. Mol. Biol.* **1998**, *279*, 665–684.
(41) Fersht, A. R. *Structure and Mechanism in Protein Science: A Guide to Enzyme Catalysis And Protein Folding*; W.H. Freeman: New York, 1999.
(42) Fan, H.; Mark, A. E.; Zhu, J.; Honig, B. *Proc. Natl. Acad. Sci. U.S.A.* **2005**, *102*, 6760–6764.
(43) Chellgren, B. W.; Creamer, T. P. *Proteins* **2006**, *62*, 411–420.
(44) Jarymowycz, V. A.; Stone, M. J. *Chem. Rev.* **2006**, *106*, 1624–1671.
(45) Zidek, L.; Novotny, M. V.; Stone, M. J. *Nat. Struct. Biol.* **1999**, *6*, 1118–1121.
(46) Glover, J. R.; Kowal, A. S.; Schirmer, E. C.; Patino, M. M.; Liu, J. J.; Lindquist, S. *Cell* **1997**, *89*, 811–819.
(47) Zurdo, J.; Guijarro, J. I.; Jimenez, J. L.; Saibil, H. R.; Dobson, C. M. *J. Mol. Biol.* **2001**, *311*, 325–340.
(48) Jimenez, J. L.; Tennent, G.; Pepys, M.; Saibil, H. R. *J. Mol. Biol.* **2001**, *311*, 241–247.
(49) Petkova, A. T.; Leapman, R. D.; Guo, Z. H.; Yau, W. M.; Mattson, M. P.; Tycko, R. *Science* **2005**, *307*, 262–265.
(50) Petkova, A. T.; Yau, W. M.; Tycko, R. *Biochemistry* **2006**, *45*, 498–512.
(51) Jimenez, J. L.; Guijarro, J. L.; Orlova, E.; Zurdo, J.; Dobson, C. M.; Sunde, M.; Saibil, H. R. *EMBO J.* **1999**, *18*, 815–821.
(52) Tattum, M. H.; Cohen-Krausz, S.; Khalili-Shirazi, A.; Jackson, G. S.; Orlova, E. V.; Collinge, J.; Clarke, A. R.; Saibil, H. R. *J. Mol. Biol.* **2006**, *357*, 975–985.
(53) Jimenez, J. L.; Nettleton, E. J.; Bouchard, M.; Robinson, C. V.; Dobson, C. M.; Saibil, H. R. *Proc. Natl. Acad. Sci. U.S.A.* **2002**, *99*, 9196–9201.
(54) van der Wel, P. C. A.; Lewandowski, J. R.; Griffin, R. G. *J. Am. Chem. Soc.* **2007**, *129*, 5117–5130.
(55) Aggeli, A.; Nyrkova, I. A.; Bell, M.; Harding, R.; Carrick, L.; McLeish, T. C. B.; Semenov, A. N.; Boden, N. *Proc. Natl. Acad. Sci. U.S.A.* **2001**, *98*, 11857–11862.
(56) Fishwick, C. W. G.; Beevers, A. J.; Carrick, L. M.; Whitehouse, C. D.; Aggeli, A.; Boden, N. *Nano Lett.* **2003**, *3*, 1475–1479.
(57) de la Paz, M. L.; Goldie, K.; Zurdo, J.; Lacroix, E.; Dobson, C. M.; Hoenger, A.; Serrano, L. *Proc. Natl. Acad. Sci. U.S.A.* **2002**, *99*, 16052–16057.
(58) Humphrey, W.; Dalke, A.; Schulten, K. *J. Mol. Graph.* **1996**, *14*, 33–38.

JP8078259